Port. Math. 82 (2025), 297–323
DOI 10.4171/PM/2144

Classification of connection graphs of global attractors for S^1-equivariant parabolic equations

Carlos Rocha

Abstract. We consider the characterization of global attractors $\mathcal{A}_f$ for semiflows generated by scalar one-dimensional semilinear parabolic equations of the form $u_t = u_{xx} + f(u, u_x)$, defined on the circle $x \in S^1$, for a class of reversible nonlinearities. Given two reversible nonlinearities, f_0 and f_1, with the same lap signature, we prove the existence of a reversible homotopy $f_\tau, 0 \le \tau \le 1$, which preserves all heteroclinic connections. Consequently, we obtain a classification of the connection graphs of global attractors in the class of reversible nonlinearities. We also describe bifurcation diagrams which reduce a global attractor $\mathcal{A}_1$ to the trivial global attractor $\mathcal{A}_0 = \{0\}$.

1. Introduction

Consider the scalar semilinear parabolic equation

$$u_t = u_{xx} + f(u, u_x), \quad x \in S^1 = \mathbb{R}/2\pi\mathbb{Z}, \tag{1.1}$$

where the nonlinearity $f : \mathbb{R}^2 \to \mathbb{R}$ is C^2 and dissipative. Sufficient dissipative conditions are boundedness, $|f(\cdot,\cdot)| \le C_0$, and a sign condition $uf(u,0) < 0$ for all large $|u| > K_0$. For less restrictive conditions see [1,32]. Then, (1.1) generates a semiflow in the Sobolev space $X = H^s(S^1)$, $s > \frac{3}{2}$, which possesses a nonempty compact *global attractor* $\mathcal{A} \subset X$. For details see [15] and also [4, 31, 32] for initial references. As general references, see [22, 33] for semiflows, and [5, 20, 21] for global attractors.

Stationary solutions of (1.1) satisfy the equation

$$0 = v_{xx} + f(v, v_x), \quad x \in S^1, \tag{1.2}$$

and are either *homogeneous equilibria* $v(t, x) = e$, where $f(e, 0) = 0$, or *nonhomogeneous stationary waves*, i.e., 2π-periodic solutions of (1.2). In general, (1.1) also

Mathematics Subject Classification 2020: 35B41 (primary); 34B15, 37G35 (secondary).
Keywords: global attractors, semilinear parabolic equations, nonlinear periodic boundary value problems.

features time periodic solutions. These are *rotating waves* $u(t,x) = v(x - ct)$, rotating around the circle S^1 with constant speed $c \neq 0$. Moreover, the nonconstant wave shapes v correspond to the 2π-periodic solutions of the ODE

$$0 = v_{xx} + f(v, v_x) + cv_x. \tag{1.3}$$

Our first assumption is

(H) all equilibria and periodic orbits of (1.1) are *hyperbolic*.

Hyperbolicity here concerns the sets of homogeneous equilibria and nonhomogeneous time periodic solutions (rotating waves) of the semilinear parabolic PDE (1.1). These are, respectively, the sets $\mathcal{E}$ and $\mathcal{P}$ which are finite due to hyperbolicity (H) and the compactness of $\mathcal{A}$, [14, 15],

$$\mathcal{E} = \{e_j : f(e_j, 0) = 0,\ 1 \leq j \leq n\},$$
$$\mathcal{P} = \{v_j(x) : v_j(0) = v_j(2\pi),\ p_j(0) = p_j(2\pi),\ x \in [0, 2\pi],\ 1 \leq j \leq q\},$$

where $p = v_x$, v_j denotes the rotating wave profiles, i.e., solutions of (1.3), and q denotes the number of nonhomogeneous periodic solutions properly x-shifted so that $v_j(0) = \min_{x \in S^1} v_j(x)$. For simplicity we include in $\mathcal{P}$ also the nonhomogeneous stationary waves. We point out that the critical solutions may have very large Morse indices $i(e_j) = \dim W^{\mathrm{u}}(e_j)$ and $i(v_j) = \dim W^{\mathrm{u}}(v_j) - 1$, see [15]. Here, $W^{\mathrm{u}}(\cdot)$ denotes the unstable manifold of an equilibrium or periodic orbit, [21, 22, 24]. In contrast, the equilibria of the related ODE (1.2), $\mathbf{e}_j = (e_j, 0)$ and $\mathbf{v}_j = (v_j, p_j)$, has only alternating saddles and centers, all in one-to-one correspondence with the equilibria of (1.1). For example, the first saddle corresponds to the first stable equilibrium $\mathbf{e}_1$ and the last saddle corresponds to the last stable equilibrium $\mathbf{e}_n$.

Notice that a nonhomogeneous stationary solution $v = v(\cdot)$ is not isolated, since all its shifted copies $v(\cdot + \vartheta)$, $\vartheta \in S^1$, are also 2π-periodic solutions of (1.2). Hence, a nonhomogeneous stationary solution is not hyperbolic in stricto sensu. To overcome this inconvenience, hyperbolicity here is understood as *normal hyperbolicity*, [16, 35], much like in the case of a periodic orbit.

The global attractor $\mathcal{A}$ is called a *Sturm attractor* (see [16]) due to the decay property (2.3) of the *zero number*, [31]. If all critical elements in $\mathcal{E} \cup \mathcal{P}$ are strictly hyperbolic, i.e., $\mathcal{P}$ does not contain nonhomogeneous stationary solutions, the Sturm attractor has the *Morse–Smale* property, [10, 25]. In this case, all the *heteroclinic orbit connections* between equilibria and periodic orbits of $\mathcal{A}$, which all together compose the global attractor, are determined by a *Sturm permutation*, [17, 35]. See also [18] for the initial results on Sturm permutations. Unfortunately, for the reversible class of nonlinearities $f(u, v) = f(u, -v)$ included in the present S^1-equivariant case, we are missing a proper Morse–Smale Theorem. Therefore, our results must be restricted to connection equivalence of global attractors postponing orbit equivalence to further research studies. This observation also applies to the statement of [35, Theorem 3] which should address connection equivalence of global attractors instead of orbit equivalence.

The phase portrait of (1.2) for a reversible nonlinearity $f(u,v) = f(u,-v)$ (even in v) has all rotating waves frozen, i.e., they are nonhomogeneous equilibria. In addition, (1.2) is *integrable* in the phase plane region corresponding to the *cyclicity set* $\mathcal{C}$, i.e., the region of all spatially periodic orbits, see [16]. Hence, for the reversible nonlinearity $f(u,u_x)$ we obtain a *period map* $T : \mathcal{D} \subset \mathbb{R} \to \mathbb{R}_+$ where the domain $\mathcal{D}$ corresponds to (the u-values) of the cyclicity set $\mathcal{C}$.

The period map $T = T(u_0)$, also called time map, is essential for the characterization of all 2π-periodic solutions of autonomous planar Hamiltonian equations, see [16, 34]. In our setting, the period map is used for the characterization of all the equilibria of (1.1), in particular, the frozen rotating waves.

Our objective is the classification of the connection graphs of all Sturm global attractors of flows generated by (1.1). This is achieved using the *lap signature class* introduced in [16,35]. The lap signature of a period map $T = T(u_0)$ consists of the set of *period lap numbers* of the 2π-periodic solutions of (1.2) endowed with a total order derived from the nesting of the periodic orbits in the phase space (v, v_x), and their *regular parenthesis structure* (called regular bracket structure in [28, 35]). We notice that the period lap number $\ell(v)$ of $v \in \mathcal{P}$ is half of the zero number: $z(v) = 2\ell(v)$, see [16]. The *lap signature class* of a period map $T = T(u_0)$ is the set of period maps with the same lap signature of $T = T(u_0)$.

Let $\mathcal{R}$ denote the space of reversible nonlinearities. Our main result asserts the following.

Theorem 1. *Let $f = f(u,u_x) \in \mathcal{R}$ and $g = g(u,u_x) \in \mathcal{R}$ denote two reversible nonlinearities with period maps in the same lap signature class. Then the corresponding global attractors are connection equivalent,*

$$\mathcal{A}_f \sim \mathcal{A}_g. \tag{1.4}$$

Here, (1.4) means connection equivalence between global attractors, [13, 14, 35]. This result is not immediate because all the critical elements in $\mathcal{P}$ fail the hyperbolicity condition (H) which would entail the automatic transversality of stable and unstable manifolds and the strong Morse–Smale property. Instead, we will address the automatic transversality of center stable and center unstable manifolds in the next Section 2. Then, Theorem 1 will follow from the next theorem.

Theorem 2. *If $f = f(u,u_x) \in \mathcal{R}$ and $g = g(u,u_x) \in \mathcal{R}$ belong to the same lap signature class (see* [16, 35]*), then there exists a global collective homotopy in $\mathcal{R}$*

between f and g which preserves hyperbolicity (H) of all the homogeneous equilibria and (normally hyperbolic) frozen rotating waves.

The construction of this *global collective homotopy* is very delicate and needs some clarification in what concerns the proof in [35], which is restricted to nonlinearities of simple type. In Section 3, we change and refine some aspects of the proof of [35, Theorem 3] making it simpler and amenable to a generalization to nonlinearities of non-simple type.

In the final Section 4, we discuss these results and conclude with the presentation of bifurcation diagrams and connection graphs of global attractors for dynamical systems generated by (1.1). We also describe bifurcation diagrams which reduce a global attractor $\mathcal{A}_1$ to the trivial global attractor $\mathcal{A}_0 = \{0\}$ by a bifurcation homotopy $f^s(u, u_x) = f(s, u, u_x) \in \mathcal{R}$ with bifurcation parameter $1 \geq s \geq 0$.

2. Transversality between center stable and center unstable manifolds

As already mentioned, the result of Theorem 1 is not immediate since all the critical elements in $\mathcal{P}$ fail the hyperbolicity condition (H). Hence, we replace stable and unstable manifolds by center stable and center unstable manifolds, and prove their automatic transversality following closely the previous transversality results established for the general problem (1.1), see [10, 15]. See also [3, 7, 23] for the original transversality results in the case of separated boundary conditions.

We recall that every 2π-periodic solution in $\mathcal{P}$ is a nonhomogeneous stationary wave frozen in time. So, let $\mathcal{F}$ denote the set of nonhomogeneous stationary waves, and $\mathcal{H}$ the set of heteroclinic orbits between equilibria, either homogeneous or nonhomogeneous. Then, for the restrictive set of reversible nonlinearities $f \in \mathcal{R}$, the global attractor $\mathcal{A}_f$ of (1.1) decomposes as

$$\mathcal{A}_f = \mathcal{E} \cup \mathcal{F} \cup \mathcal{H}.$$

By reversibility, each nonhomogeneous stationary solution $v(\cdot) \in \mathcal{F}$ generates a continuum of shifted copies $v(\cdot + \vartheta)$, $\vartheta \in S^1$, all normally hyperbolic. This implies that each $v(\cdot) \in \mathcal{F}$ has a unique center manifold composed by its frozen shifted copies. In view of the gradient flow variational character of (1.1) for $f \in \mathcal{R}$, (see [12]), non-stationary orbits $u(t, \cdot)$ converge either to equilibria or stationary waves as $t \to \pm\infty$. Hence, these orbit connections are essentially heteroclinic connections between equilibria. Moreover, the proof of this transversality was already sketched in [15, Propositions 3.1 and 3.2]. In the following, for each $v(\cdot) \in \mathcal{F}$, we let

$$W^{\mathrm{cu}}(v(\cdot)) = \bigcup_{\vartheta \in S^1} W^{\mathrm{u}}(v(\cdot + \vartheta)), \quad W^{\mathrm{cs}}(v(\cdot)) = \bigcup_{\vartheta \in S^1} W^{\mathrm{s}}(v(\cdot + \vartheta)).$$

Finally, we recall that the existence of heteroclinic orbits between two critical elements in $\mathcal{E} \cup \mathcal{F}$ is determined by a convenient notion of *adjacency* between these elements, see [15, Theorems 1.3 and 1.4].

Proof of Theorem 1. In the following, we consider only the case of orbit connections between nonhomogeneous stationary waves since the remaining cases are simpler.

We say that two (different) stationary waves $v_\pm(\cdot) \in \mathcal{F}$ are connected by a heteroclinic orbit $u(t, \cdot)$ if this connecting orbit converges to suitably phase shifted stationary waves $v_\pm^\infty := v_\pm(\cdot + \vartheta_\pm)$ as $t \to \pm\infty$ for some fixed $\vartheta_\pm \in \mathbb{R}$.

We introduce here the following definition:

(D) We say that $W^{\mathrm{cu}}(v_-)$ and $W^{\mathrm{cs}}(v_+)$ are transverse,

$$W^{\mathrm{cu}}(v_-) \,\overline{\pitchfork}\, W^{\mathrm{cs}}(v_+), \tag{2.1}$$

if their intersection is empty, or if the strongly unstable manifold $W^{\mathrm{u}}(v_-^\infty)$ and the strongly stable manifold $W^{\mathrm{s}}(v_+^\infty)$ are *codimension one transverse*, i.e., at intersection points their tangential spaces span a codimension one subspace $X_1 \subset X$.

Let $u_0 = u(0, \cdot)$ denote the initial condition of the connecting orbit. Then, if $\mathcal{S}(t) : X \to X$ denotes the semiflow generated by (1.1), we have that $u(t, x) = \mathcal{S}(t)u_0(x)$. Moreover, if $D\mathcal{S}(t)$ is the Fréchet derivative of $\mathcal{S}(t)$, then for any $w_0 \in X$ the curve $w(t, \cdot) = (D\mathcal{S}(t)u_0(\cdot))w_0(\cdot)$ in X defines the classical solution $w(t, x)$ of the linearized equation

$$w_t = w_{xx} + f_p(u, u_x)w_x + f_u(u, u_x)w, \quad x \in S^1,\ t > 0, \quad w(0, x) = w_0(x). \tag{2.2}$$

In abstract form, this is a linear evolution equation $\dot{w} = A(t)w$ which generates a solution operator $w = \mathcal{T}(t, \tau)w_\tau$, $t \geq \tau$. Note that $\mathcal{T}(t, \tau)$ is injective (see, for example, [10]).

We recall that, for the solution $w(t, \cdot)$ of (2.2), we have the well-known monotone nonincreasing property of the zero number

$$t \mapsto z(w(t, \cdot)), \quad \text{is monotone nonincreasing,} \tag{2.3}$$

(see [30, Lemma 2.6]). Moreover, the zero number strictly decreases at multiple zeros of $w(t, \cdot)$, (see [2]).

For $u = v_\pm^\infty$, equation (2.2) denotes the linearization around the equilibria $v_\pm^\infty \in \mathcal{F}$ and is autonomous. The corresponding autonomous linear evolution equations with linear operators $A^\pm$ generate semigroups $\mathcal{T}^\pm(t)$, $t \geq 0$, which are analytic. We next collect some information regarding the spectral properties of $A^\pm$.

The spectrum of $A^{\pm}$ is the set of eigenvalues of the second order differential eigenvalue problem with periodic boundary conditions

$$w_{xx} + f_p(u,u_x)w_x + f_u(u,u_x)w = \lambda w, \quad x \in S^1, \tag{2.4}$$

with $u = v^{\infty}_{\pm} \in \mathcal{F}$. Let $\operatorname{spec}(A^{\pm}) = \{\lambda^{\pm}_j\}^{\infty}_{j=0}$ denote the set of eigenvalues of (2.4) numbered according to $\lambda^{\pm}_0 > \operatorname{Re}\lambda^{\pm}_1 \geq \operatorname{Re}\lambda^{\pm}_2 \geq \cdots$. By standard spectral theory for (2.4), see, for example, [9], the eigenvalue sequences are partially ordered by

$$\operatorname{Re}\lambda^{\pm}_{2j} > \operatorname{Re}\lambda^{\pm}_{2j+1}, \quad j = 0, 1, 2, \ldots$$

As a simple remark we point out that, if $\operatorname{Re}\lambda^{\pm}_{2j-1} > \operatorname{Re}\lambda^{\pm}_{2j}$ for any $j \geq 1$, then the eigenvalues $\{\lambda^{\pm}_{2j-1}, \lambda^{\pm}_{2j}\}$ are real.

Let $E^{\pm}_0$ denote the eigenspaces of constant functions corresponding to $\lambda^{\pm}_0$, and let $E^{\pm}_j$ denote the generalized eigenspaces corresponding to the spectral sets $\{\lambda^{\pm}_{2j-1}, \lambda^{\pm}_{2j}\}$ for $j \geq 1$. Then, each $w \in E^{\pm}_j \setminus \{0\}$ has only simple zeros on S^1 and $z(w) = 2j$, [4, 32].

Let $u_0 \in W^{\mathrm{u}}(v^{\infty}_{-}) \cap W^{\mathrm{s}}(v^{\infty}_{+})$. Then $u(t,\cdot) \to v^{\infty}_{\pm}$ as $t \to \pm\infty$ and the linearization (2.2) around the equilibria $v^{\infty}_{\pm} \in \mathcal{F}$ correspond to the asymptotic behaviors of (2.2) around $u(t,\cdot)$.

Let $T_{u_0}W^{\mathrm{s}}(v^{\infty}_{\pm})$ and $T_{u_0}W^{\mathrm{u}}(v^{\infty}_{\pm})$ denote the tangent manifolds at u_0 of the stable and unstable manifolds of $v^{\infty}_{\pm}$. By the S^1-equivariance of (1.1) these linear manifolds are subspaces of a codimension one subspace $X_1 \subset X$. In fact, for $\vartheta \in S^1$ let R_ϑ denote the S^1-action induced by the x-shift $(R_\vartheta u)(x) = u(x+\vartheta)$. Hence, we have

$$\frac{d}{d\vartheta}(R_\vartheta u_0)(x)|_{\vartheta=0} = \frac{d}{d\vartheta}u_0(x+\vartheta)|_{\vartheta=0} = (u_0)_x(x). \tag{2.5}$$

Let $X_0 \subset X$ denote the one-dimensional linear subspace generated by (2.5), $X_0 = \operatorname{span}\{(u_0)_x\}$. Since $(u_0)_x \notin (T_{u_0}W^{\mathrm{s}}(v^{\infty}_{\pm}) \cup T_{u_0}W^{\mathrm{u}}(v^{\infty}_{\pm}))$, this implies

$$X_0 \cap T_{u_0}W^{\mathrm{s}}(v^{\infty}_{\pm}) = X_0 \cap T_{u_0}W^{\mathrm{u}}(v^{\infty}_{\pm}) = \{0\}.$$

Moreover, $T_{u_0}W^{\mathrm{s}}(v^{\infty}_{\pm})$ and $T_{u_0}W^{\mathrm{u}}(v^{\infty}_{\pm})$ span a codimension one subspace X_1. Since $\dim X_0 = 1$, we obtain

$$X_0 + X_1 = X. \tag{2.6}$$

This also holds for each equilibrium $v \in \mathcal{F}$ with $X_0 = \operatorname{span}\{v_x\}$, and in particular for the equilibria $v^{\infty}_{\pm}$.

By normal hyperbolicity of the nonhomogeneous stationary wave $v \in \mathcal{F}$, we define its Morse index $i(v)$ as the number m of eigenvalues with strictly positive real part $\operatorname{Re}\lambda_j > 0$. Then, for $i(v) = m$, $\lambda_{m+1} = 0$ corresponds to the eigenfunction $v_{m+1} = v_x(x)$, and we obtain

$$\dim W^{\mathrm{cu}}(v) = i(v) + 1, \quad \operatorname{codim} W^{\mathrm{cs}}(v) = i(v).$$

As in [10] (for periodic orbits), two cases need to be considered. If the Morse index is odd, $i(v) = 2N-1$, then the eigenspace $E_N = E_N^{\pm}$ corresponds to the spectral set $\{\lambda_{2N-1}^{\pm} = 0, \lambda_{2N}^{\pm}\}$. If on the other hand the Morse index is even, $i(v) = 2N$, then the eigenspace E_N corresponds to the spectral set $\{\lambda_{2N-1}^{\pm}, \lambda_{2N}^{\pm} = 0\}$. In each case, let P_0 denote the projection onto the eigenspace corresponding to the zero eigenvalue, i.e., $P_0 X = \operatorname{span}\{v_x\} \subset E_N$. Then, for each $w \in P_0 X \setminus \{0\}$ we have $z(w) = 2N$ and, by the monotone nonincreasing property of the zero number (2.3), we obtain

$$\begin{aligned} z(v_0) &\leq \begin{cases} 2N-2 = i(v)-1 & \text{if } i(v) = 2N-1, \\ 2N = i(v) & \text{if } i(v) = 2N, \end{cases} \quad \text{for } v_0 \in W^{\mathrm{u}}(v), \\ z(v_0) &\geq \begin{cases} 2N = i(v)+1 & \text{if } i(v) = 2N-1, \\ 2N+2 = i(v)+2 & \text{if } i(v) = 2N, \end{cases} \quad \text{for } v_0 \in W^{\mathrm{s}}(v). \end{aligned} \tag{2.7}$$

Now assume the existence of an intersection point u_0 between the unstable manifold of v_-^{∞} and the stable manifold of v_+^{∞},

$$u_0 \in W^{\mathrm{u}}(v_-^{\infty}) \cap W^{\mathrm{s}}(v_+^{\infty}) \subset W^{\mathrm{cu}}(v_-) \cap W^{\mathrm{cs}}(v_+).$$

Since the connecting orbit $u(t,\cdot)$ with $u(0,\cdot) = u_0$ lies in $W^{\mathrm{u}}(v_-^{\infty}) \cap W^{\mathrm{s}}(v_+^{\infty})$, the invariance of these manifolds implies that

$$u_t(t,\cdot) \in T_{u_0} W^{\mathrm{u}}(v_-^{\infty}) \cap T_{u_0} W^{\mathrm{s}}(v_+^{\infty}).$$

Moreover, since $u_t(0,\cdot)$ is nonzero, the monotone nonincreasing property (2.3) of the zero number implies

$$2i(v_+^{\infty}) < z(u_t(0,\cdot)) \leq 2i(v_-^{\infty}). \tag{2.8}$$

Then, combining the inequalities (2.7), we obtain the following result.

Lemma 1. *If* $u_0 \in (W^{\mathrm{u}}(v_-^{\infty}) \cap (W^{\mathrm{s}}(v_+^{\infty}))) \setminus \{v_-^{\infty}, v_+^{\infty}\}$ *and* $2N^{\pm} = z(v_{\pm}^{\infty})$, *then*

$$N^- \geq N^+ \quad \text{and} \quad i(v_-^{\infty}) \geq i(v_+^{\infty}) + 1. \tag{2.9}$$

Moreover, if $i(v_+^{\infty}) = 2N^+$, *then* $N^- \geq N^+ + 1$.

Notice that (2.9) prevents the existence of homoclinic orbits to the set of frozen shifted copies of equilibria in $\mathcal{F}$.

For the proof of transversality we adapt the proof in [10] and use [7] (in particular, its Theorem 3.1 and the results of Appendix B).

For any $\psi \in X$ we define

$$\nu_{\infty}(\psi) := \limsup_{n\to\infty} \operatorname{Re} \log \|\mathcal{T}(n,0)\psi\|^{\frac{1}{n}}.$$

The number $\nu_{\infty}(\psi)$ denotes the *Lyapunov characteristic number* for the equation (2.2) with $u = u(t,\cdot)$.

For any integer $j \geq 0$ we define the spaces

$$F_j^+ := \{\psi \in X : \nu_\infty(\psi) \leq r_j\},$$

where, to respect the spectral set pairs $\{\lambda_{2j-1}^+, \lambda_{2j}^+\}$ in $\sigma(A^+)$, we let $r_0 = \lambda_0^+$ and $r_j = \operatorname{Re} \lambda_{2j-1}^+$, $j \geq 1$. Then, we have

$$X = F_0^+ \supset F_1^+ \supset F_2^+ \supset \cdots, \quad \bigcap_{j=0}^{\infty} F_j^+ = \{0\}.$$

Assuming that $\nu_\infty(\psi) \in \{r_j, r_{j+1}\}$ with odd j, then $\psi \in F_j^+ \setminus F_{j+1}^+$ and we consider the asymptotic behavior of $v(n, \psi) = \mathcal{T}(n, 0)\psi$, $n \in \mathbb{N}$, obtaining for some subsequence $k_n \in \mathbb{N}$

$$\lim_{n\to\infty} \frac{v(k_n, \psi)}{\|v(k_n, \psi)\|} = \phi,$$

with ϕ in the norm one sphere in X. This shows that

$$z(\psi) \geq z(v(k_n, \psi)) \geq z\Big(\frac{v(k_n, \psi)}{\|v(k_n, \psi)\|}\Big) = z(\phi).$$

Next, we use the asymptotic behavior of $v(k_n, \psi)$ to characterize the zero number $z(\psi)$ of the initial condition ψ. We first address the zero number characterization of solutions on the stable manifold of the target equilibrium v_+^∞.

Again we need to consider the alternatives for the even/odd parity of the index j of the eigenvalues λ_j, $j \geq 1$. If j is even, i.e., the eigenspace $E_{\frac{j}{2}}^+$ corresponds to the spectral set $\{\lambda_{j-1}^+, \lambda_j^+\}$, then $\psi \in F_{\frac{j}{2}}^+ \setminus F_{\frac{j}{2}+1}^+$ and there exists an asymptotic $\phi \in E_{\frac{j}{2}}^+$ such that $z(\psi) \geq z(\phi) = j$. If, on the other hand, j is odd, i.e., the eigenspace $E_{\frac{j+1}{2}}^+$ corresponds to the spectral set $\{\lambda_j^+, \lambda_{j+1}^+\}$, then $\psi \in F_{\frac{j+1}{2}}^+ \setminus F_{\frac{j+1}{2}+1}^+$ and there exists an asymptotic $\phi \in E_{\frac{j+1}{2}}^+$ such that $z(\psi) \geq z(\phi) = j + 1$.

Note that $T_{u_0} W^{\mathrm{s}}(v_+^\infty) = \{\psi \in X : \nu_\infty(\psi) < 0\}$. To continue, let $i(v_+^\infty) = 2N^+$ be even. Then $r_{N^+} = \lambda_{2N^+}^+ = 0$ and for a sufficiently large $m \in \mathbb{N}$ we have

$$T_{u(m,u_0)} W^{\mathrm{s}}(v_+^\infty) = F_{N^+}^+,$$

which is isomorphic to

$$\mathrm{cl}_X(E_{N^+}^+ \oplus E_{N^++1}^+ \oplus \cdots).$$

In this case, we conclude that $z(\psi) \geq 2N^+ + 2$ for $v \in T_{u(m,u_0)} W^{\mathrm{s}}(v_+^\infty) \setminus \{0\}$ and $\operatorname{codim} T_{u(m,u_0)} W^{\mathrm{s}}(v_+^\infty) = 2N^+ + 1$.

Before considering the alternative of odd $i(v_+^\infty) = 2N^+ - 1$ we define

$$F_{\lambda_{2N^+}}^+ := \{\psi \in X : \nu^\infty(\psi) < 0\}.$$

Hence, if $i(v_+^\infty) = 2N^+ - 1$ is odd, then $r_{N^+} < \lambda^+_{2N^+-1} = 0$ and for a sufficiently large $m \in \mathbb{N}$ we have $T_{u(m,u_0)} W^s(v_+^\infty) = F^+_{\lambda_{2N^+}}$, which is isomorphic to

$$\mathrm{cl}_X(\mathrm{span}\{w^+_{2N^++1}\} \oplus E^+_{N^+} \oplus E^+_{N^++1} \oplus \cdots). \tag{2.10}$$

We conclude that $z(\psi) \geq 2N^+$ for $v \in T_{u(m,u_0)} W^s(v_+^\infty) \setminus \{0\}$ and

$$\mathrm{codim}\, T_{u(m,u_0)} W^s(v_+^\infty) = 2N^+.$$

Since $T_{u_0} W^s(v_+^\infty)$ is the preimage of $T_{u(m,u_0)} W^s(v_+^\infty)$ under the injective semiflow $\mathcal{T}(m,0)$ we obtain the following result.

Lemma 2. *Assume $\psi \in T_{u_0} W^s(v_+^\infty) \setminus \{0\}$. Then we have the following alternative:*

$$\begin{cases} z(\psi) \geq 2N^+ + 2 & \textit{and} \quad \mathrm{codim}\, T_{u_0} W^s(v_+^\infty) = 2N^+ + 1 & \textit{if } i(v_+^\infty) = 2N^+, \\ z(\psi) \geq 2N^+ & \textit{and} \quad \mathrm{codim}\, T_{u_0} W^s(v_+^\infty) = 2N^+ & \textit{if } i(v_+^\infty) = 2N^+ - 1. \end{cases} \tag{2.11}$$

Finally, we address the zero number characterization of solutions on the unstable manifold of the source equilibrium v_-^∞. We invoke the backward unique continuation of the semiflow $\mathcal{T}(m,0)$, $m \in \mathbb{N}$, and use the semiflow $\mathcal{T}(-m,0)$, which is well defined on the unstable manifold $W^u(v_-^\infty)$. Let $i(v_+^\infty) = 2N^+$ be even. Then, by Lemma 1 we have $N^- \geq N^+ + 1$ and, for sufficiently large $m \in \mathbb{N}$, there is a subspace $W_{-m} \subset T_{u(-m,u_0)} W^u(v_-^\infty)$ such that $z(v) \leq 2N^+$ for $v \in W_{-m}$. This implies that, for $W_m := \mathcal{T}(m,-m) W_{-m}$, we have $z(v) \leq 2N^+$ for $v \in W_m \setminus \{0\}$. In view of Lemma 2, this shows that $W_m \cap W^s(v_+^\infty) = \{0\}$ which implies $W_m \subseteq T_{u(m,u_0)} W^u(v_+^\infty)$. Therefore, for $m \in \mathbb{N}$ sufficiently large, W_m is isomorphic to

$$E_0^+ \oplus \cdots \oplus E^+_{N^+-1} \oplus \mathrm{span}\{w^+_{2N^+-1}\},$$

where $w^+_{2N^+-1}$ is an eigenfunction associated to the (real) eigenfunction $\lambda^+_{2N^+-1}$. This shows that

$$\dim W_{-m} = \dim W_m = 2N^+, \quad \text{and} \quad z(v) \leq 2N^+,\ v \in W_{-m} \setminus \{0\}.$$

Alternatively, let $i(v_+^\infty) = 2N^+ - 1$ be odd. By (2.9) we have $N^- \geq N^+$ and, as in the previous case, for sufficiently large $m \in \mathbb{N}$ there is a subspace $W_{-m} \subset T_{u(-m,u_0)} W^u(v_-^\infty)$ such that $z(v) \leq 2N^+ - 2$ for $v \in W_{-m}$. This shows that $z(v) \leq 2N^+ - 2$ for $v \in W_m \setminus \{0\}$, where $W_m := \mathcal{T}(m,-m) W_{-m}$ is isomorphic to

$$E_0^+ \oplus \cdots \oplus E^+_{N^+-1}.$$

This implies that

$$\dim W_{-m} = \dim W_m = 2N^+ - 1, \quad \text{and} \quad z(v) \leq 2N^+ - 2,\ v \in W_{-m} \setminus \{0\}.$$

In summary, we obtained the following result.

Lemma 3. *There is a subspace* $W_0 = \mathcal{T}(0, -m)W_{-m} \subset T_{u_0}W^{\mathrm{u}}(v_-^\infty)$ *with* $\dim W_0 = i(v_+^\infty)$ *such that, if* $\psi \in W_0 \setminus \{0\}$*, then the following alternative holds:*

$$\begin{cases} z(\psi) \le 2N^+ & \text{if } i(v_+^\infty) = 2N^+, \\ z(\psi) \le 2N^+ - 2 & \text{if } i(v_+^\infty) = 2N^+ - 1. \end{cases} \tag{2.12}$$

The automatic transversality of center stable and center unstable manifolds, claimed in the next Theorem 3, is now obtained from the combination of Lemmas 2 and 3. Note that this transversality implies the preservation of heteroclinic orbit connections in the S^1-equivariant case and entails the connection equivalence (1.4) asserted by Theorem 1. ■

Theorem 3. *Let* $v_\pm \in \mathcal{F}$ *denote normally hyperbolic fixed points of the semigroup* $\mathcal{S}(t)$ *generated by* (1.1)*. Then the center unstable manifold of* v_-*,* $W^{\mathrm{cu}}(v_-)$*, and the center stable manifold of* v_+*,* $W^{\mathrm{cs}}(v_+)$*, intersect transversely,*

$$W^{\mathrm{cs}}(v_+) \pitchfork W^{\mathrm{cu}}(v_-). \tag{2.13}$$

Proof of Theorem 3. Recall that if $W^{\mathrm{cu}}(v-) \cap W^{\mathrm{cs}}(v_+) = \emptyset$ then $W^{\mathrm{cu}}(v_-)$ and $W^{\mathrm{cs}}(v_+)$ are transverse by definition (D). So, we assume the existence of an intersection point u_0 between the center unstable manifold of v_- and the center stable manifold of v_+.

Then, by (2.12) for $w \in W_0 \setminus \{0\} \subset T_{u_0}W^{\mathrm{u}}(v_-^\infty) \setminus \{0\}$ and (2.11) for $w \in T_{u_0}W^{\mathrm{s}}(v_+^\infty) \setminus \{0\}$ we obtain

$$W_0 \cap T_{u_0}W^{\mathrm{s}}(v_+^\infty) = \{0\}.$$

Moreover, the combination of (2.11) and (2.12) implies

$$\dim W_0 = \operatorname{codim} T_{u_0}W^{\mathrm{s}}(v_+^\infty) - 1.$$

This shows that

$$W_0 \oplus T_{u_0}W^{\mathrm{s}}(v_+^\infty) = \widetilde{X}_1,$$

where $\widetilde{X}_1 \subset X$ has $\operatorname{codim} \widetilde{X}_1 = 1$. Since $W_0 \subset T_{u_0}W^{\mathrm{u}}(v_-^\infty)$, this implies $W^{\mathrm{u}}(v_-^\infty) \pitchfork W^{\mathrm{s}}(v_+^\infty)$ and, by our definition (D), this shows the transversality result (2.13) and completes the proof of Theorem 3.

To finish, let $\widetilde{X}_0$ denote the one-dimensional complement of $\widetilde{X}_1$, i.e., $\widetilde{X}_0 + \widetilde{X}_1 = X$, obtained by using again the backward linear flow generated by (2.2) with $u = u(t, \cdot)$. Then, we have

$$T_{u_0}W^{\mathrm{u}}(v_-^\infty) + T_{u_0}W^{\mathrm{s}}(v_+^\infty) + \widetilde{X}_0 = X,$$

concluding this discussion of transversality. ■

Notice that forty years ago Dan Henry [23] used the expression “amazing” to refer to this type of result, and advised the reader to “look at it again”!

3. Homotopy construction

We first consider the obstructions to the homotopy construction between a reversible nonlinearity $f_0 = f_0(u, u_x)$ and an $f_1 = f_1(u)$ in the class of Hamiltonian systems.

Let $T = T(u_0) : \mathcal{D} \to \mathbb{R}_+$ denote the period map of a reversible nonlinearity $f = f(u, u_x)$. By continuity, we extend $\mathcal{D}$ to $u_0 = e$ corresponding to the center $(e, 0)$ which is encircled by periodic orbits. For simplicity, by a translation $u \mapsto u - e$ we let $e = 0$.

A necessary and sufficient condition for $T = T(u_0)$ to be realizable by a Hamiltonian nonlinearity $g = g(u)$ is

(C) $d(u_0 T(u_0))/du_0 > 0$, $u_0 \in \mathcal{D}$.

For references see [36, Theorem 4.2.5 and Proposition 4.2.6], [37, Theorem 5], [18, Theorem 4.2], and [34, Section 4].

We first show the existence of reversible nonlinearities $f = f(u, u_x)$ for which this condition is not satisfied. For this purpose, consider the nonlinearity

$$f(u, u_x) = \frac{k}{2} u \Big(k u^2 + \sqrt{k^2 u^4 + 4 u_x^2} \Big). \tag{3.1}$$

Each level curve of the first integral $I(u, v) = \frac{1}{2}(k u^2 + \sqrt{k^2 u^4 + 4 v^2})$ of (1.2) is an ellipse $v^2 + k I_0 u^2 = I_0^2$ where $I_0 := I(u_0, 0) = k u_0^2$. Therefore, the period map for this nonlinearity is given by

$$T(u_0) = 4 \int_0^{u_0} \frac{du}{k \sqrt{u_0^4 - u_0^2 u^2}} = \frac{2\pi}{k |u_0|}, \qquad u_0 \neq 0.$$

Hence, since $d(u_0 T(u_0))/du_0 = 0$ for $u_0 \neq 0$, condition (C) is not satisfied.

If the period map $T(u_0)$ satisfies condition (C) we are able to find a Hamiltonian pendulum nonlinearity $g = g(u)$ with the same period map, [34]. See also [36, 37] for the preliminary results. In this case, the convex combination

$$f_\tau(u, u_x) = (1 - \tau) f(u, u_x) + \tau g(u) \tag{3.2}$$

provides the desired *pendulum realization homotopy* in the Hamiltonian class of nonlinearities.

On the other hand, the failing of condition (C) prevents the homotopy in the Hamiltonian class since the period map is not realizable in this class. Therefore, the homotopy has to be constructed directly in $\mathcal{R}$ using the phase portrait of (1.2). We define the *Hamiltonian realization homotopy* as a continuous transformation of the cyclicity set $\mathcal{C}$ of $f(u, u_x)$, which preserves the hyperbolicity of all homogeneous equilibria and frozen rotating waves, and shrinks the period map along the u-axis until it satisfies condition (C).

Let $K = (n-1)/2 + r$ denote the number of connected regions of the cyclicity set $\mathcal{C}$. Here n denotes the odd number of equilibria and r the number of annular regions. Annular regions are the multiply connected regions bounded by two saddles and their homoclinic ODE separatrices (see, for example, the region $\mathcal{C}_1$ in Figure 6). Notice that each equilibrium of (1.1) corresponds to a center or a saddle point of the phase portrait of (1.2). The centers and saddles alternate for increasing values of u_0, starting and ending with saddles. Then $(n-1)/2$ is the number of punctured disks encircling the centers. Moreover, r is the number of annular regions which surround more than one single center. This implies that $0 \leq r \leq (n-3)/2$. See [16].

Finally, a reversible nonlinearity $f = f(u, u_x)$ is of *simple type* if $r = 0$, i.e., if there are no annular regions. This is a slightly more restrictive definition then the one used in [35]. If $r = 0$ then each 2π-periodic orbit of (1.2) encircles exactly one center in the phase plane (v, v_x).

Then, let $g = g(u)$ denote a Hamiltonian nonlinearity with period map $T = T(u_0)$, and let G denote the potential function of (1.2), i.e., $G' = g$. Under the hyperbolicity assumption (H) for (1.1) with $f = f_1(u, u_x)$, all the zeros of g are non-degenerate (i.e., $g(u_0) = 0$ implies $g'(u_0) \neq 0$). Moreover, the period map $T = T(u_0)$ satisfies the nondegeneracy condition: $T(u_0) = \frac{2\pi}{k}$ implies $T'(u_0) \neq 0$ for all positive integers $k \in \mathbb{N}$. See [34] for details.

For simplicity, we make here the generic assumption

(M) the potential function G is a *Morse function*.

Hence, in addition to the nondegeneracy of the zeros of g, we also assume that all the critical values of G are distinct ($g(u_0) = g(u_1) = 0$ implies $G(u_0) \neq G(u_1)$). Since we can always add a small perturbation to f_1, this generic assumption does not affect our result.

Initially, we consider that the lap signature class of $f(u, u_x)$ is of simple type. This implies that $r = 0$ and we deal with a cyclicity set composed only of isolated punctured disks around the centers in the phase portrait.

Proof of Theorem 2. The proof essentially consists on the construction of a Hamiltonian realization homotopy in $\mathcal{R}$ between $f_0(u, u_x)$ and a nonlinearity $f_1(u, u_x)$ satisfying condition (C) of a Hamiltonian nonlinearity $g = g(u)$. This homotopy preserves: (a) hyperbolicity of all critical elements of the flow generated by (1.1) with $f = f_0(u, u_x)$; and hence, (b) the lap signature of the period map $T = T_f$.

We consider first the case of a single connected cyclicity set $\mathcal{C}_0$ surrounding a unique center, *Case (I)*, and then we consider the case of multiple isolated punctured disks, *Case (II)*. Later on we will treat the case of nonlinearities with lap signature class of non-simple type.

Case (I): $n = 3$ and $r = 0$. For the reversible nonlinearity $f = f_0(u, u_x)$ let $e_1 < e_2 = 0 < e_3$ denote the three zeros of $f_0(\cdot, 0)$ corresponding to two saddle points, $\mathbf{e}_1, \mathbf{e}_3$, and a center at the origin $\mathbf{e}_2 = (0, 0)$. The boundary $\partial\mathcal{C}_0$ of the cyclicity set is given by a saddle point and an orbit homoclinic to this saddle. Without loss of generality we assume that the saddle point is $\mathbf{e}_1$. Therefore, the cyclicity set $\mathcal{C}_0$ is positioned to the right of $\mathbf{e}_1$, see Figure 1.

For simplicity we define the interval (a^-, a^+) corresponding to the u-values of the cyclicity set $\mathcal{C}_0$. Here $a^- := e_1$ and a^+, $0 < a^+ < e_3$, corresponds to the maximum u-value of the homoclinic orbit. Then, the period map for $f_0(u, u_x)$ satisfies $T : (a^-, 0) \cup (0, a^+) \to \mathbb{R}$ and we extend the domain of $T(u_0)$ to $u_0 = 0$ by continuity. By the hyperbolicity assumption (H) and the smoothness of $f_0(u, u_x)$ we obtain

$$T(0) \in \left(\frac{2\pi}{k}, \frac{2\pi}{k-1}\right) \text{ for some } k \in \mathbb{N}, \text{ and } T'(0) = 0,$$

see, for example, [36].

Assume the set of periodic solutions $\mathcal{P}$ to be nonempty, i.e., $q \geq 1$. We recall that the frozen rotating waves of $f_0(u, u_x)$ are the 2π-periodic solutions of (1.2), $\mathbf{v}_j \in \mathcal{P}$ for $1 \leq j \leq q$. Let $a_j = \min_{x \in [0, 2\pi]} v_j(x)$ denote the minimal initial values of the u-coordinates of these 2π-periodic solutions. Then, we have $a^- < a_1 < \cdots < a_q < 0$ and for each $1 \leq j \leq q$ we have $T(a_j) = \frac{2\pi}{k_j}$ for some $k_j \in \mathbb{N}$.

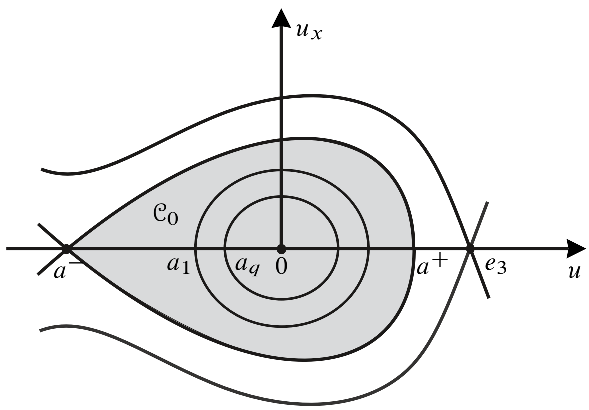

Figure 1. Cyclicity set $\mathcal{C}_0$ in the case of $n = 3, r = 0$ and with $q = 2$ 2π-periodic orbits.

The proof of *Case (I)* then proceeds by the construction of a homotopy between f_0 and a reversible f_1 which preserves hyperbolicity (H) and for which the period map $T = T_1(a)$ satisfies condition (C). This involves the use of a local diffeomorphism of the plane (u, u_x) which preserves the period map values. Based on [15, Lemma 5.1], this diffeomorphism is described in [35, Section 5], and is recalled here for the benefit of the reader.

Let $(v, p(v)) = (v(\cdot, a), p(v(\cdot, a))$ denote the periodic orbits of (1.2) on the phase plane (u, u_x) where $v = v(\cdot, a)$ denotes the solution with $v(0, a) = a$, $v_x(0, a) > 0$. On the cyclicity set $\mathcal{C}_0$ we define the scaling map

$$\Phi(v, p) = \Omega(v, p)(v, p)$$

where $\Omega : \mathcal{C}_0 \to \mathbb{R}$ is constant along the periodic orbits of (1.2), i.e.,

$$\Omega(v(\cdot, a), p(v(\cdot, a))) = \Omega(a, 0).$$

Then, let $\omega : (0, a^+) \to \mathbb{R}$ denote the scale function $\omega(a) = \Omega(a, 0)$ which is assumed monotone nondecreasing in order to have Φ as a diffeomorphism on the cyclicity set $\mathcal{C}_0$. We extend the domain of ω to the interval (a^-, a^+) using the minimal values of the periodic orbits in the cyclicity set and defining $\omega(0) := \omega(0^+) = \omega(0^-)$. Finally, we extend the diffeomorphism Φ to the whole phase space $(u, u_x) \in \mathbb{R}^2$ by defining Φ as the identity in $\mathbb{R}^2 \setminus \mathcal{C}_0$.

To define the scale function $\omega|_{(0,a^+)}$, let $c_1, c_2 \in (\alpha_1, a^+)$ denote two constants satisfying $\alpha_1 < c_1 < c_2 < a^+$, where again α_1 denotes the maximal value of the outermost 2π-periodic solution $v_1(\cdot, a_1)$. Recall that $\lim_{a \to a^+} T(a) = +\infty$, hence $T(a) > 2\pi$ for $a \in (\alpha_1, a^+)$, see Figure 2. Changing the phase portrait of (1.2) in a small neighborhood of the homoclinic orbit to $\mathbf{e}_1$ does not affect the global attrac-

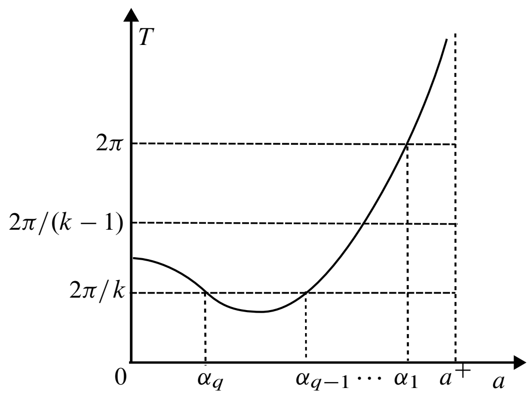

Figure 2. Graph of the period map $T = T(a)$ on the half interval $(0, a^+)$. Here, $\alpha_j = \max_{x \in [0,2\pi]} v_j(x, a_j)$, $j = 1, \ldots, q$, denote the maximal values of the 2π-periodic solutions.

tor $\mathcal{A}_f$. Therefore, we can assume that the period map satisfies $\lim_{a\to a^+} T(a) = +\infty$ monotonically. Hence, we have $T'(a) > 0$ in a neighborhood of a^+ and we always choose c_1 in this neighborhood. Then, for a parameter $\delta \in (0,1)$, we define

$$\omega(a) = \begin{cases} \delta & \text{for } a \in (0, c_1), \\ C^2\text{-smooth monotone increasing} & \text{for } a \in [c_1, c_2], \\ 1 & \text{for } a \in (c_2, a^+). \end{cases} \tag{3.3}$$

Therefore, with this scale function ω, the diffeomorphism Φ shrinks all the 2π-periodic orbits to a neighborhood of the origin as δ decreases, see Figure 3. Since the scaling of the period map preserves the nondegeneracy of the points corresponding to the maximal values of the 2π-periodic solutions, their hyperbolicity is preserved by the scaling. Moreover, the period map $T_1(a)$ satisfies

$$T_1(a) = T(\omega(a)a). \tag{3.4}$$

Hence, we obtain

$$\frac{d}{da}(aT_1(a)) = T(\omega(a)a) + (\omega(a) + a\omega'(a))aT'(\omega(a)a). \tag{3.5}$$

Notice that $\omega'(a) = 0$ for all $a > 0$ except $a \in (c_1, c_2)$ where $\omega'(a) > 0$ and, by our choice of c_1 in a neighborhood of a^+, the period map satisfies $T'(\omega(a)a) > 0$ there. This implies that, for δ sufficiently small, $T_1(a)$ satisfies condition (C). We conclude that $f_1(u, u_x)$ is realizable in the Hamiltonian class of nonlinearities completing the proof of *Case (I)*.

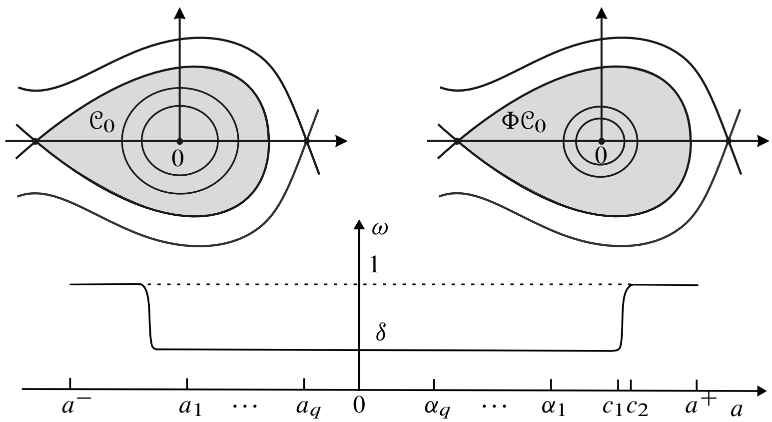

Figure 3. Upper left: Cyclicity set $\mathcal{C}_0$ for $f = f_0(u, u_x)$. Upper right: Cyclicity set $\Phi\mathcal{C}_0$ for $f = f_1(u, u_x)$. Bottom: Graph of the scale function ω.

Case (II): $n \geq 5$ and $r = 0$. Now we deal with a cyclicity set

$$\mathcal{C} = \bigcup_{1 \leq k \leq (n-1)/2} \mathcal{C}_k$$

composed of several punctured disks surrounding the $(n-1)/2$ centers of (1.2), see Figure 4. Since each $\mathcal{C}_k$ is isolated (by condition (M) and the simple type $r = 0$), the proof in this case follows by repeating the previous procedure in each region $\mathcal{C}_k$, $k = 1, \ldots, (n-1)/2$. Therefore, we obtain $(n-1)/2$ disjoint graphs of Hamiltonian realizations, one for each region $\mathcal{C}_k$. Then, a Hamiltonian $g(u)$ which realizes $f_1(u, u_x)$ is obtained by extending the domain to $\mathbb{R}$ joining these g graphs. For this extension, we fill the $(n-3)/2$ closed interval gaps with C^2-smooth functions without introducing further zeros of g. Similarly, in the two remaining unbounded intervals, our extension choice is such that no further zeros are introduced. Finally, we choose a globally bounded extension $g : \mathbb{R} \to \mathbb{R}$.

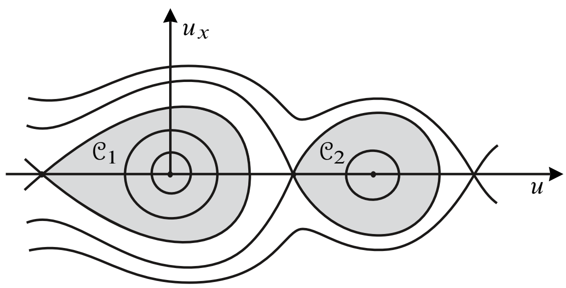

Figure 4. Cyclicity set $\mathcal{C} = \mathcal{C}_1 \cup \mathcal{C}_2$ for $f = f_0(u, u_x)$ with $n = 5$ and $r = 0$.

Clearly, $f_0(u, u_x)$ and $g(u)$ belong to the same lap signature class. Then, the desired Hamiltonian realization homotopy has the form (see [35]),

$$f_\tau(v, p) = \Omega_\tau(v, p)(f_0 \circ \Phi_\tau^{-1}(v, p)), \quad 0 \leq \tau \leq 1, \tag{3.6}$$

where

$$\Phi_\tau(v, p) = \Omega_\tau(v, p)\,(v, p), \quad \Omega_\tau(a, 0) = \omega_\tau(a), \quad \omega_\tau = (1-\tau) + \tau\omega, \tag{3.7}$$

followed by the pendulum realization homotopy (3.2) between $f_1(u, u_x)$ and $g(u)$. This completes the proof of *Case (II)*.

Remark: Consider again the Hamiltonian realization of $f = f_0(u, u_x)$ by $g(u)$ in *Case (I)*. The cyclicity set $\mathcal{C}_0$ is *right oriented* if its boundary $\partial\mathcal{C}_0$ contains the saddle point $\mathbf{e}_1$, i.e., $a^- = e_1$. Similarly, $\mathcal{C}_0$ is *left oriented* if $\partial\mathcal{C}_0$ contains the saddle point

$\mathbf{e}_3$, i.e., $a^+ = e_3$. Then, if $\mathcal{C}_0$ is right oriented, the nonlinearity g satisfies $g(a^-) = g(e_1) = 0$ and is negative for $u \in (a^-, 0)$ and positive for $u \in (0, a^+)$. Therefore, the extension of g to the interval gap (a^+, e_3) is also positive. On the other hand, if $\mathcal{C}_0$ is left oriented, we have $g(e_2) = g(a^+) = 0$ and the extension of g to the interval gap (e_1, a^-) is negative. This holds in the multiple *Case (II)* for all the isolated components $\mathcal{C}_k$ of the cyclicity set.

Due to the integrability and the simple type of f_0 the phase portrait of (1.2) for $f = f_0(u, u_x)$ has the following characteristic. There is a saddle point $\mathbf{e}_m$, $1 \leq m \leq n$ and odd, such that all $\mathcal{C}_k$ to the left of $\mathbf{e}_m$ are right oriented, and all $\mathcal{C}_k$ to the right of $\mathbf{e}_m$ are left oriented. See Figure 5.

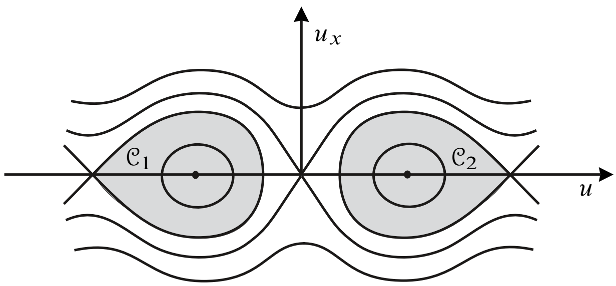

Figure 5. Cyclicity set $\mathcal{C} = \mathcal{C}_1 \cup \mathcal{C}_2$ for $f = f_0(u, u_x)$ with $n = 5$, $r = 0$ and $m = 3$. The previous Figure 4 illustrates the case $m = n = 5$.

The phase portrait of (1.2) for $f = g(u)$ depends essentially on the singular values of the potential function

$$G(a) = \int_{e_2}^{a} g(s)ds \tag{3.8}$$

at the saddle points, i.e., the local maxima of G, and not on the Morse type of G. Indeed, the Morse type of G is easily modified by changing the values of the extended g in its $(n-1)/2$ closed interval gaps.

Since all $\mathcal{C}_k$ are right oriented at the left of $\mathbf{e}_m$ and left oriented at the right, all the extensions of g are positive to the left of e_m and negative to the right. Then, by (3.8), $\mathbf{e}_m$ is the saddle point with the maximum value $G(e_m) = \max\{G(e_{2k-1}) : 1 \leq k \leq (n+1)/2\}$ and the sequence of singular values $G(e_{2k-1})$ satisfies the inequalities

$$G(e_1) < \cdots < G(e_m), \quad G(e_m) > \cdots > G(e_n). \tag{3.9}$$

This ensures that the phase portraits of (1.2) for $f = f_0(u, u_x)$ and $f = g(u)$ are qualitatively the same.

We now prove the generalization of our main result to the case of nonlinearities with lap signature of non-simple type. We prove this following the same approach used in the previous *Cases (I)* and *(II)*. We first consider the case of $\mathcal{C}$ with a single outermost annular region $\mathcal{C}_1$ surrounding two cyclicity sets $\mathcal{C}_2 \cup \mathcal{C}_3 = \mathcal{C} \setminus \mathcal{C}_1$, *Case (III)*, and then we consider the case of multiple outermost annular regions of $\mathcal{C}$ and punctured disks, *Case (IV)*.

In view of the proof of previous cases, we only need to consider nonlinearities $f_0(u, u_x)$ of non-simple type, $r \geq 1$. This implies $n \geq 5$. As before we construct a Hamiltonian realization homotopy in $\mathcal{R}$ between $f_0(u, u_x)$ and a nonlinearity $f_1(u, u_x)$ satisfying condition (C).

Case (III): $n = 5$ and $r = 1$. In this case, the phase portrait of (1.2) for $f = f_0(u, u_x)$ has three cyclicity regions. In addition to two punctured disks $\mathcal{C}_2$, $\mathcal{C}_3$ surrounding the centers $\mathbf{e}_2$, $\mathbf{e}_4$, there is an annular region $\mathcal{C}_1$ surrounding both punctured disks. This implies that the saddle point $\mathbf{e}_3$ has two homoclinic orbits composing the boundary $\partial(\mathcal{C}_2 \cup \mathcal{C}_3)$. The cyclicity regions $\mathcal{C}_2$ and $\mathcal{C}_3$ have opposite left/right orientations and the homoclinic orbits form an ∞ shaped curve. See Figure 6.

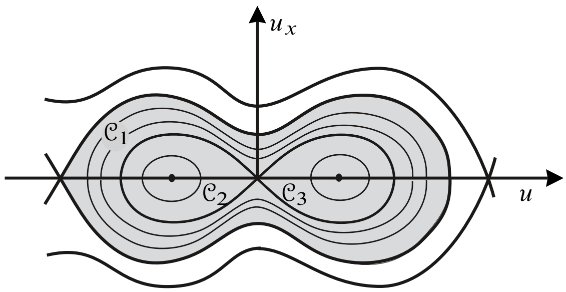

Figure 6. Cyclicity set $\mathcal{C} = \mathcal{C}_1 \cup \mathcal{C}_2 \cup \mathcal{C}_3$ for $f = f_0(u, u_x)$ with $n = 5$, $r = 1$ and $q = 4$. Two of these 2π-periodic orbits are in the annular region $\mathcal{C}_1$.

By a translation in u, we assume here that $e_3 = 0$. Therefore, the $n = 5$ equilibria of (1.1) for $f = f_0(u, u_x)$ satisfy $e_1 < e_2 < e_3 = 0 < e_4 < e_5$. We use the same notation that was used in the previous cases. Specifically, we let $(a^-, 0) = (e_1, 0)$ denote the first saddle point, and $(a^+, 0)$ the maximum value of the orbit homoclinic to $(e_1, 0)$. Moreover, we denote by $a_1, \dots, a_{q_1}$ the Neumann initial values of the 2π-periodic orbits $v_j \in \mathcal{P}$ in the annular region $\mathcal{C}_1$, i.e., $a_j = \min_{x \in [0,2\pi]} v_j$, $1 \leq j \leq q_1$. Similarly, we denote by $\alpha_1, \dots, \alpha_{q_1}$ the corresponding maximum values $\alpha_j = \max_{x \in [0,2\pi]} v_j$, $1 \leq j \leq q_1$. Notice that in annular regions $\mathcal{C}_k$ the numbers q_k are always even, see [16].

The proof follows the same argument employed in *Case (I)*. We use again a shrinking scale function ω which grants the Hamiltonian realization of (3.3) for $f = f_1(u, u_x)$. The essential difference here is the shrinking of all equilibria and 2π-periodic orbits in $\mathcal{C}$ to a neighborhood of the middle saddle point $\mathbf{e}_3$ instead of a neighborhood of the center $\mathbf{e}_2$.

Then, let again c_1, c_2 denote the two constants satisfying $\alpha_1 < c_1 < c_2 < a^+$ (c_1 in the appropriate neighborhood of a^+) and, for $\delta \in (0,1)$, define the scale function ω by (3.3). Once more, using this scale function ω, we define the diffeomorphism $\Phi : \mathcal{C} \to \mathcal{C}$ which we extend to $\mathrm{cl}\,\mathcal{C}$ by continuity, and to the phase plane $\mathbb{R}^2$ by the identity, $\Phi|_{(\mathbb{R}^2 \setminus \mathrm{cl}\,\mathcal{C})} = \mathrm{id}$.

As expected, Φ shrinks all equilibria and 2π-periodic orbits in $\mathcal{C}$ to a neighborhood of the origin $(e_3, 0) = (0,0)$ as δ decreases, preserving hyperbolicity, see Figure 7. In addition, under Φ the period map T_1 obtained from the period map T of (1.2) for $f = f_0(u, u_x)$ satisfies (3.4). Then, from (3.5) we again conclude that $T_1(a)$ satisfies condition (C). Hence, $f_1(u, u_x)$ is realizable by a Hamiltonian nonlinearity $g(u)$ and the desired homotopy from $f_1(u, u_x)$ to $g(u)$ has the form (3.6), (3.7), which is followed by the pendulum realization homotopy (3.2). This completes the proof in *Case (III)*.

Case (IV): $n \geq 7$ and $r \geq 1$. We proceed sequentially, following the total order imposed by the regular parenthesis structure of the cyclicity regions. For example, the regular parenthesis structure of the cyclicity region shown in Figure 6 is

$$(()()). \tag{3.10}$$

The use of the regular parenthesis structure of the cyclicity regions instead of the 2π-periodic orbits is necessary to overcome the case of $r \geq 1$ without 2π-periodic orbits in some annular region $\mathcal{C}_k$, i.e., $q_k = 0$.

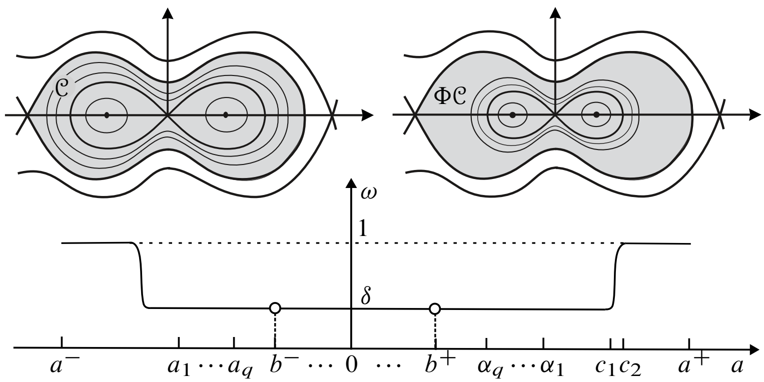

Figure 7. Upper left: Cyclicity set $\mathcal{C}$ for $f = f_0(u, u_x)$. Upper right: Cyclicity set $\Phi\mathcal{C}$ for $f = f_1(u, u_x)$. Bottom: Graph of the scale function ω. Here b^- and b^+ denote respectively the minimum and maximum u-values of the orbits homoclinic to the origin. The white balls correspond to these homoclinic orbits, and $b^\pm \notin \mathcal{D}$ since the homoclinic orbits are not in $\mathcal{C}$. Also note that $0 \notin \mathcal{D}$.

We initially consider the first region $\widetilde{\mathcal{C}}$ which may contain the first and outermost 2π-periodic orbit corresponding to the solution with minimal value $a_1 = \min_{x\in[0,2\pi]} v_1(x, a_1)$. If $\widetilde{\mathcal{C}}$ is an isolated punctured disk we apply the scale shrinking procedure described in *Case (II)*. So, next we assume that $\widetilde{\mathcal{C}}$ is an annular region.

We let $\mathcal{C}$ denote the union of $\widetilde{\mathcal{C}}$ with all the cyclicity regions that it encloses. Then, we apply the same argument used in *Case (III)* shrinking all equilibria and 2π-periodic orbits contained in $\mathcal{C}$ to a neighborhood of the unique saddle point in the inner boundary of $\widetilde{\mathcal{C}}$. For example, in Figure 6 the saddle point is $\mathbf{e}_3$. Therefore, using the same notation as in *Case (III)*, we obtain a diffeomorphism $\Phi : \mathcal{C} \to \mathcal{C}$ which preserves hyperbolicity and leads to a period map $T_1|_{(a^-,a^+)}$ satisfying condition (C).

Let κ denote the number of annular regions and punctured disks with an outermost homoclinic orbit in their boundaries. Let $\widetilde{\mathcal{C}}_k$ denote these either punctured disks or outermost annular regions of the cyclicity set $\mathcal{C}$. If $\widetilde{\mathcal{C}}_k$ is a punctured disk we define $\mathcal{C}_k := \widetilde{\mathcal{C}}_k$. If $\widetilde{\mathcal{C}}_k$ is an annular region we define $\mathcal{C}_k = \widetilde{\mathcal{C}}_k \cup \overline{\mathcal{C}}_k$ where $\overline{\mathcal{C}}_k$ denotes the union of all the cyclicity sets encircled by $\widetilde{\mathcal{C}}_k$. In this way we obtain a sequence $\mathcal{C}_1, \ldots, \mathcal{C}_\kappa$ were we can apply repeatedly the above procedure. Therefore, we obtain

$$\mathcal{C} = \bigcup_{1\le k\le\kappa} \mathcal{C}_k$$

with diffeomorphism $\Phi : \mathcal{C} \to \mathcal{C}$ which preserves hyperbolicity. Moreover, the period maps $T_1(a)$ restricted to the intervals defined by the maximal homoclinic u-values satisfy condition (C) for δ sufficiently small.

Hence, we again extend Φ to $\mathrm{cl}\,\mathcal{C}$ by continuity and to the complete phase space $(u, u_x) \in \mathbb{R}^2$ by the identity $\Phi|_{(\mathbb{R}^2\setminus \mathrm{cl}\,\mathcal{C})} = \mathrm{id}$. Notice that each $\mathcal{C}_k$ is isolated and, due to this isolation and the integrability of (1.1) for $f = f_1(u, u_x)$, each $\mathcal{C}_k$ accepts the left/right orientation described in the previous remark after *Case (II)*.

We obtain a Hamiltonian and pendulum realization of (1.2) for $f = f_1(u, u_x)$ by a nonlinearity $g(u)$ defined on the isolated intervals determined by the regions $\mathcal{C}_k$. Then, after the C^2 smooth and globally bounded extension of $g(u)$ to $\mathbb{R}$, filling the unbounded intervals and the interval gaps, we define the potential G by (3.8). Therefore, due to the partial order (3.9) restricted to the saddle points on the boundaries of $\mathcal{C}_k$, the phase portraits of (1.2) for $f = f_0(u, u_x)$ and $f = g(u)$ are qualitatively the same. Then, preservation of hyperbolicity ensures that $f = f_0(u, u_x)$ and $f = g(u)$ belong to the same lap signature class. This completes the proof of *Case (IV)*.

Finally, as a result of [35, Theorem 2] (see also [16, 34]), there exists a homotopy between the pendulum realization $g(u)$ of $f_0(u, u_x)$ and a pendulum realization $\overline{g}(u)$ of $f_1(u, u_x)$ since, by assumption, both belong to the same lap signature class. In fact, all global attractors of pendulum realizations with the same lap signature are connection equivalent.

In summary, the global collective homotopy is the composition of:

(i) a Hamiltonian realization homotopy (3.6), (3.7), and a pendulum realization homotopy (3.2) from $f_0(u, u_x)$ to $g(u)$;

(ii) a homotopy between $g(u)$ and $\overline{g}(u)$;

(iii) a reverse pendulum realization homotopy and a reverse Hamiltonian realization homotopy from $\overline{g}(u)$ to $f_1(u, u_x)$.

This concludes the proof of Theorem 2. ∎

4. Discussion and concluding remarks

Theorem 1 is a contribution to the geometric and qualitative theory of dynamical systems generated by parabolic partial differential equations. This result, applied to one-dimensional scalar semilinear PDEs, extends to the case of reversible nonlinearities the classification of these dynamical systems, already initiated in [15–17, 34]. Similar results are also available in the more complex case of monotone feedback delay differential equations. For results and references see [26, 27, 29].

Clearly, due to Theorem 1, a classification of the global attractors for dynamical systems generated by (1.1) in the reversible class of nonlinearities is provided by the lap signature class. As mentioned in Section 1, the lap signature class is given by the set of period lap numbers of the 2π-periodic orbits endowed with the total order derived from the regular parenthesis structure of their nesting in phase space (u, u_x). This has the form (see [16])

$$\big(\{\ell_1^1, \dots, \ell_{k_1}^1\}(\{\ell_1^2, \dots, \ell_{k_2}^2\}(\cdots)\cdots(\{\ell_1^K, \dots, \ell_{k_K}^K\}))\big),$$

where K again denotes the number of cyclicity regions, k_j denotes the number of 2π-periodic orbits in the jth annular or punctured disk region (this may be empty, in which case $k_j = 0$), and ℓ_i^j denotes the period lap number of the ith 2π-periodic orbit in the jth cyclicity region. The regular parenthesis structure represents the nesting of the periodic orbits. To illustrate this representation, we exhibit the lap signature class for the example of Figure 6 (with $n = 5$, $r = 1$, $k_1 = 2$ and $k_2 = k_3 = 1$) completing the parenthesis order structure shown in (3.10),

$$\big(\{1, 1\}(\{1\})(\{1\})\big).$$

The present result also shows that in the class of S^1-equivariant nonlinearities $f^s(u, u_x) = f(s, u, u_x)$, $s \in [0, 1]$ there is a continuous family of functions f^s, $s \in [0, 1]$, connecting the global Sturm attractors $\mathcal{A}_{f^0} = \{\mathbf{0}\}$ and $\mathcal{A}_{f^1}$ through a finite number of local (degenerate) bifurcations. Here s denotes the bifurcation parameter. Moreover, these bifurcations consist only of pitchfork and Hopf bifurcations.

Notice that the bifurcations shown are degenerate because the family $f^s \in \mathcal{R}$, $s \in [0,1]$, is entirely constructed in the symmetry class of reversible nonlinearities $f = f(u, u_x)$, which implies its integrability. We also illustrate this bifurcation diagram in the example of Figure 6. We obtain a family f^s, $s \in [0,1]$, with six bifurcations points at $s = k/7$, $1 \le k \le 6$, and seven (degenerate) structurally stable regions $[0,1] \setminus (\bigcup_{1 \le k \le 6} \{k/7\})$. In Figure 8, we illustrate the period maps in these seven regions. Since we are restricted to the integrable case $f^s \in \mathcal{R}$, all the bifurcations are degenerate. For general references see [6, 8, 19].

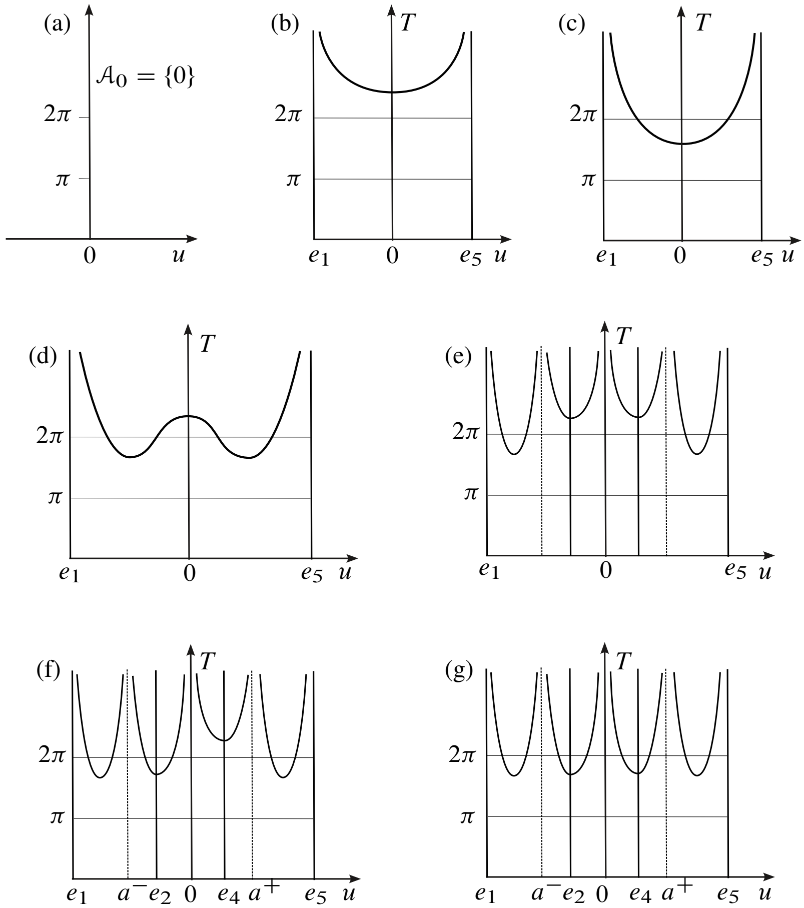

Figure 8. For the global attractor $\mathcal{A}_1$ of (1.1) with lap signature $(\{1,1\}(\{1\})(\{1\}))$, we consider the family $f_s \in \mathcal{R}$, $s \in [0,1]$ connecting $\mathcal{A}_0 = \{0\}$ to $\mathcal{A}_1$. For this example we illustrate the seven period maps which satisfy condition (H). The corresponding s-intervals are: (a) $0 < s < 1/7$; (b) $1/7 < s < 2/7$; (c) $2/7 < s < 3/7$; (d) $3/7 < s < 4/7$; (e) $4/7 < s < 5/7$; (f) $5/7 < s < 6/7$; and, (g) $6/7 < s < 1$. The occurring six bifurcations are discussed in Figure 9.

In Figure 9, we then show the bifurcation diagram from $\mathcal{A}_0 = \{0\}$ to $\mathcal{A}_1$ and the connection graph of a nondegenerate global attractor $\mathcal{A}_{s>1}$ of (1.1) homotopic to the (degenerate) $\mathcal{A}_1$. For this we extend the family f^s to $s > 1$, connecting the reversible (degenerate) $\mathcal{A}_1$ to a global attractor $\mathcal{A}_{s>1}$ which is not reversible, see [16]. In this case, $\mathcal{A}_{s>1}$ is nondegenerate and we have the usual notions of stability of equilibria and rotation waves, [17]. See [15, Proposition 3.1] and [17, Theorem 10].

The global attractor $\mathcal{A}_{s>1}$ has three stable equilibria, denoted by $\{\mathbf{e}_1, \mathbf{e}_3 = \mathbf{0}, \mathbf{e}_5\}$, and two unstable equilibria, $\{\mathbf{e}_2, \mathbf{e}_4\}$, where

$$\dim W^{\mathrm{u}}(\mathbf{e}_1) = \dim W^{\mathrm{u}}(\mathbf{e}_3) = \dim W^{\mathrm{u}}(\mathbf{e}_5) = 0,$$
$$\dim W^{\mathrm{u}}(\mathbf{e}_2) = \dim W^{\mathrm{u}}(\mathbf{e}_4) = 3.$$

In addition, there are four rotating waves, denoted $\{\mathbf{v}_1, \mathbf{v}_2, \mathbf{v}_3, \mathbf{v}_4\}$ (by order of appearance). By the normal hyperbolicity of rotating waves, we obtain

$$\dim W^{\mathrm{u}}(\mathbf{v}_1) = \dim W^{\mathrm{u}}(\mathbf{v}_3) = \dim W^{\mathrm{u}}(\mathbf{v}_4) = 1, \quad \dim W^{\mathrm{u}}(\mathbf{v}_2) = 2.$$

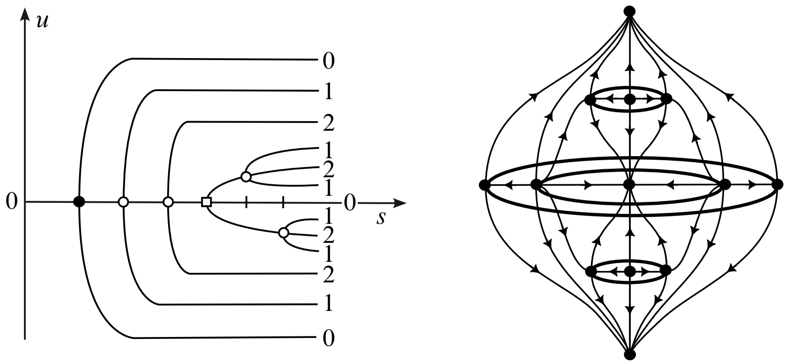

Figure 9. *Left:* The bifurcation diagram for the reversible family $f^s \in \mathcal{R}$, $s \in [0, 1]$, (see Figure 8). The bifurcation points are, respectively: a pitchfork of a stable saddle point (black ball); degenerate Hopf bifurcations (white balls); and, a pitchfork of centers (white square). Moreover, the sequence of bifurcations leading to $\mathcal{A}_1$ are: (i) a supercritical pitchfork bifurcation of two stable saddle points at $s = 1/7$; (ii) a supercritical Hopf bifurcation of an unstable 2π-periodic orbit at $s = 2/7$; (iii) a supercritical Hopf bifurcation of an unstable 2π-periodic orbit at $s = 3/7$; (iv) a supercritical pitchfork bifurcation of two centers at $s = 4/7$: (v) a supercritical Hopf bifurcation of an unstable 2π-periodic orbit at $s = 5/7$ in the upper branch center; and, (vi) a supercritical Hopf bifurcation of an unstable 2π-periodic orbit at $s = 6/7$ in the lower branch center. At the right margin of the bifurcation diagram we indicate the Morse indices corresponding to the equilibria and rotating waves of the nondegenerate Neumann section of the global attractor $\mathcal{A}_{s>1}$. *Right:* The connection graph of the nondegenerate global attractor $\mathcal{A}_{s>1}$.

Therefore, since

$$\dim \mathcal{A}_{s>1} = \max\big\{\dim W^{\mathrm{u}}(\mathbf{e}_j), 1 + \dim W^{\mathrm{u}}(\mathbf{v}_k), 1 \leq j \leq 5, 1 \leq k \leq 4\big\} = 3,$$

the global attractor $\mathcal{A}_{s>1}$ is three-dimensional. The heteroclinic orbit connections follow from the connections on the Neumann section of $\mathcal{A}_{s>1}$, [15, 17]. The rotating waves, each one rotating with its own fixed speed c_j, appear on the slow stable/unstable invariant manifolds of the equilibria $\{\mathbf{e}_2, \mathbf{e}_3, \mathbf{e}_4\}$.

We conclude by observing that the connection equivalence of global attractors presented in Theorem 1 extends to the general non-reversible case as orbit equivalence, if we assume that all spatially nonhomogeneous solutions of (1.1) are rotating waves, rotating around the circle S^1 with constant speeds $c_j \neq 0$. In this case, we have $\mathcal{F} = \emptyset$ and all periodic orbits in $\mathcal{P}$ are rotating waves. So, in addition to Theorem 1, we can invoke hyperbolicity (H) and the strong Morse–Smale property.

As a final comment, we believe that Theorem 1 holds for orbit equivalence. To support this statement we observe that a small perturbation $h(u, u_x) = \varepsilon v_x$ breaks reversibility and the orbit equivalence statement holds for the homotopy with $f + h$.

As an application we exhibit the connection graph of the global attractor of (1.1) for the S^1-equivariant but non-reversible perturbed Chafee–Infante nonlinearity,

$$u_t = u_{xx} + \lambda u - u^3 + \varepsilon u_x, \quad x \in S^1, t \geq 0, \tag{4.1}$$

where $\lambda > 0$ satisfies $\lambda \neq \lambda_k := k^2, k \in \mathbb{N}$, and $\varepsilon \neq 0$. The set of equilibria of (4.1), $\mathcal{E} = \{\mathbf{e}_1, \mathbf{e}_2, \mathbf{e}_3\}$, has the equilibria $\mathbf{e}_1 = +\sqrt{\lambda}$ and $\mathbf{e}_3 = -\sqrt{\lambda}$, which are defined and hyperbolic for all $\lambda > 0$. These are saddle points of (1.2). The third equilibrium, $\mathbf{e}_2 = 0$, is also hyperbolic for $\lambda \neq \lambda_1, \lambda_2, \ldots$, and is a center of (1.2).

For $\lambda \in (\lambda_k, \lambda_{k+1})$ the set of periodic orbits $\mathcal{P} = \{v_1, \ldots, v_k\}$ has k hyperbolic rotating waves which rotate around S^1 with speed ε and $\mathcal{F} = \emptyset$. Hence, the lap signature of the global attractor $\mathcal{A}_\lambda$ is

$$(\{1, \ldots, k\}),$$

and the connection graph of $\mathcal{A}_\lambda$ is shown in Figure 10. As expected, the connection graph of this "spindle attractor" with multiple periodic orbits in his "belt" is a tower, see [11]. By the previous results using normal hyperbolicity this connection graph is preserved for $\varepsilon = 0$, i.e., the reversible case.

As a concluding remark we point out that the nonlinearity $f = f(u, u_x)$ can be regarded as a feedback control parameter for the reaction-diffusion equation (1.1). This provides a very interesting model for certain applications. We mention, for example, the possibility of stabilizing certain equilibria corresponding to reaction-diffusion patterns in chemical reactors with a proper choice of a nonlinearity $f = f(u, u_x)$.

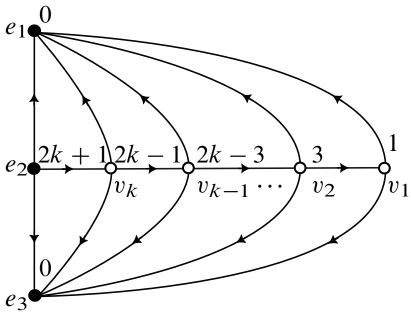

Figure 10. Connection graph of the global attractor $\mathcal{A}_\lambda$ of (4.1) for $k^2 < \lambda < (k+1)^2$. The numbers close to the vertices are the corresponding Morse indices. This shows that $\dim \mathcal{A}_\lambda = 2k+1$.

Acknowledgments. The author acknowledges the continuous support of Bernold Fiedler (Freie U. Berlin). I am deeply thankful for his longtime friendship and collaboration. I am also grateful to the continuous support of Isabel Rocha. Without her constant support, this endeavor would not be possible.

The author also acknowledges a helpful discussion with Luis Barreira, and the expert comments of the three anonymous referees which largely contributed to the improvement of the manuscript.

Funding. This work was partially supported by FCT/Portugal through the project UIDB/04459/2020 with DOI identifier 10-54499/UIDP/04459/2020.

References

[1] H. Amann, Global existence for semilinear parabolic systems. *J. Reine Angew. Math.* **360** (1985), 47–83 Zbl 0564.35060 MR 0799657

[2] S. Angenent, The zero set of a solution of a parabolic equation. *J. Reine Angew. Math.* **390** (1988), 79–96 Zbl 0644.35050 MR 0953678

[3] S. B. Angenent, The Morse–Smale property for a semilinear parabolic equation. *J. Differential Equations* **62** (1986), no. 3, 427–442 Zbl 0581.58026 MR 0837763

[4] S. B. Angenent and B. Fiedler, The dynamics of rotating waves in scalar reaction diffusion equations. *Trans. Amer. Math. Soc.* **307** (1988), no. 2, 545–568 Zbl 0696.35086 MR 0940217

[5] A. V. Babin and M. I. Vishik, *Attractors of evolution equations*. Stud. Math. Appl. 25, North-Holland Publishing Co., Amsterdam, 1992 Zbl 0778.58002 MR 1156492

[6] J. Carr, *Applications of centre manifold theory*. Appl. Math. Sci. 35, Springer, New York-Berlin, 1981 Zbl 0464.58001 MR 0635782

[7] M. Chen, X.-Y. Chen, and J. K. Hale, Structural stability for time-periodic one-dimensional parabolic equations. *J. Differential Equations* **96** (1992), no. 2, 355–418 Zbl 0779.35061 MR 1156666

[8] S. N. Chow and J. K. Hale, *Methods of bifurcation theory*. Grundlehren Math. Wiss. 251, Springer, New York-Berlin, 1982 Zbl 0487.47039 MR 0660633

[9] E. A. Coddington and N. Levinson, *Theory of ordinary differential equations*. McGraw-Hill Book Co., Inc., New York-Toronto-London, 1955 Zbl 0064.33002 MR 0069338

[10] R. Czaja and C. Rocha, Transversality in scalar reaction-diffusion equations on a circle. *J. Differential Equations* **245** (2008), no. 3, 692–721 Zbl 1157.35004 MR 2422524

[11] R. De Leo and J. A. Yorke, The graph of the logistic map is a tower. *Discrete Contin. Dyn. Syst.* **41** (2021), no. 11, 5243–5269 Zbl 1484.37028 MR 4305584

[12] B. Fiedler, K. Grotta-Ragazzo, and K. Rosha, An explicit form of Lyapunov function for mirror-symmetric parabolic partial differential equations on the circle. *Uspekhi Mat. Nauk* **69** (2014), no. 3(417), 27–42, English translation: *Russ. Math. Surveys.*, **69** (2014), 419-433 Zbl 1307.35058 MR 3287503

[13] B. Fiedler and C. Rocha, Heteroclinic orbits of semilinear parabolic equations. *J. Differential Equations* **125** (1996), no. 1, 239–281 Zbl 0849.35056 MR 1376067

[14] B. Fiedler and C. Rocha, Orbit equivalence of global attractors of semilinear parabolic differential equations. *Trans. Amer. Math. Soc.* **352** (2000), no. 1, 257–284 Zbl 0932.37065 MR 1475682

[15] B. Fiedler, C. Rocha, and M. Wolfrum, Heteroclinic orbits between rotating waves of semilinear parabolic equations on the circle. *J. Differential Equations* **201** (2004), no. 1, 99–138 Zbl 1064.35076 MR 2057540

[16] B. Fiedler, C. Rocha, and M. Wolfrum, A permutation characterization of Sturm global attractors of Hamiltonian type. *J. Differential Equations* **252** (2012), no. 1, 588–623 Zbl 1233.35042 MR 2852219

[17] B. Fiedler, C. Rocha, and M. Wolfrum, Sturm global attractors for S^1-equivariant parabolic equations. *Netw. Heterog. Media* **7** (2012), no. 4, 617–659 Zbl 1262.35053 MR 3004679

[18] G. Fusco and C. Rocha, A permutation related to the dynamics of a scalar parabolic PDE. *J. Differential Equations* **91** (1991), no. 1, 111–137 MR 1106120

[19] J. Guckenheimer and P. Holmes, *Nonlinear oscillations, dynamical systems, and bifurcations of vector fields*. Appl. Math. Sci. 42, Springer, New York, 1983 Zbl 0515.34001 MR 0709768

[20] J. K. Hale, *Asymptotic behavior of dissipative systems*. Math. Surveys Monogr. 25, American Mathematical Society, Providence, RI, 1988 Zbl 0642.58013 MR 0941371

[21] J. K. Hale, L. T. Magalhães, and W. M. Oliva, *Dynamics in infinite dimensions*. Second edn., Appl. Math. Sci. 47, Springer, New York, 2002 Zbl 1002.37002 MR 1914080

[22] D. Henry, *Geometric theory of semilinear parabolic equations*. Lecture Notes in Math. 840, Springer, Berlin-New York, 1981 Zbl 0456.35001 MR 0610244

[23] D. B. Henry, Some infinite-dimensional Morse–Smale systems defined by parabolic partial differential equations. *J. Differential Equations* **59** (1985), no. 2, 165–205 Zbl 0572.58012 MR 0804887

[24] M. W. Hirsch, C. C. Pugh, and M. Shub, *Invariant manifolds*. Lecture Notes in Math., Vol 583, Springer, Berlin-New York, 1977 Zbl 0355.58009 MR 0501173

[25] R. Joly and G. Raugel, Generic Morse–Smale property for the parabolic equation on the circle. *Ann. Inst. H. Poincaré C Anal. Non Linéaire* **27** (2010), no. 6, 1397–1440 Zbl 1213.35046 MR 2738326

[26] T. Krisztin and G. Vas, Large-amplitude periodic solutions for differential equations with delayed monotone positive feedback. *J. Dynam. Differential Equations* **23** (2011), no. 4, 727–790 Zbl 1247.34120 MR 2859940

[27] T. Krisztin and G. Vas, The unstable set of a periodic orbit for delayed positive feedback. *J. Dynam. Differential Equations* **28** (2016), no. 3-4, 805–855 Zbl 1361.34082 MR 3537356

[28] S. K. Lando and A. K. Zvonkin, *Graphs on surfaces and their applications*. Encyclopaedia Math. Sci. 141, Springer, Berlin, 2004 Zbl 1040.05001 MR 2036721

[29] A. López Nieto, *Enharmonic motion: towards the global dynamics of negative delayed feedback*. Ph.D. thesis, Freie Universität Berlin, 2023, https://refubium.fu-berlin.de/handle/fub188/40322 visited on 5 June 2025

[30] H. Matano, Nonincrease of the lap-number of a solution for a one-dimensional semilinear parabolic equation. *J. Fac. Sci. Univ. Tokyo Sect. IA Math.* **29** (1982), no. 2, 401–441 Zbl 0496.35011 MR 0672070

[31] H. Matano, Asymptotic behavior of solutions of semilinear heat equations on S^1. In *Nonlinear diffusion equations and their equilibrium states, II (Berkeley, CA, 1986)*, pp. 139–162, Math. Sci. Res. Inst. Publ. 13, Springer, New York, 1988 Zbl 0671.35039 MR 0956085

[32] H. Matano and K.-I. Nakamura, The global attractor of semilinear parabolic equations on S^1. *Discrete Contin. Dynam. Systems* **3** (1997), no. 1, 1–24 Zbl 0949.35022 MR 1422536

[33] A. Pazy, *Semigroups of linear operators and applications to partial differential equations*. Appl. Math. Sci. 44, Springer, New York, 1983 Zbl 0516.47023 MR 0710486

[34] C. Rocha, Realization of period maps of planar Hamiltonian systems. *J. Dynam. Differential Equations* **19** (2007), no. 3, 571–591 Zbl 1149.34004 MR 2350239

[35] C. Rocha, Orbit equivalence of global attractors for S^1-equivariant parabolic equations. *São Paulo J. Math. Sci.* **6** (2012), no. 2, 365–374 Zbl 1302.35065 MR 3135646

[36] R. Schaaf, *Global solution branches of two-point boundary value problems*. Lecture Notes in Math. 1458, Springer, Berlin, 1990 Zbl 0780.34010 MR 1090827

[37] M. Urabe, Relations between periods and amplitudes of periodic solutions of $\ddot{x} + g(x) = 0$. *Funkcial. Ekvac.* **6** (1964), 63–88 Zbl 0127.04502 MR 0173820

Received 3 May 2024; revised 21 March 2025.

Carlos Rocha
Centro de Análise Matemática, Geometria e Sistemas Dinâmicos, Departamento de Matemática, Instituto Superior Técnico, Universidade de Lisboa, Av. Rovisco Pais 1, 1049–001 Lisbon, Portugal; crocha@tecnico.ulisboa.pt